Optical Memory and Spatial Chaos

W. J. Firth
Strathclyde University, Glasgow, Scotland
(Received 11 January 1988)

The steady states of an array of bistable optical elements are analyzed by the use of a nonlinear-dynamics analogy. Spatial chaos is an essential counterpart of effective optical-memory action. Criteria for stability and maximum packing density are obtained.

PACS numbers: 42.65.Bp, 05.45.+b

Optical bistability (OB) has been intensively investigated in recent years,[1,2] partly at least because of the possibility of the employment of OB devices as memory or switching elements in optical computers or processors. Chaos, both dynamical[3] and spatial,[4] has similarly attracted attention, both for its fundamental interest as complexity generated from simple laws and for its ubiquity. This work establishes a connection between optical memory and spatial chaos in a reasonably simple case which invites generalization. This connection is of interest because it brings to optical memory and related systems the powerful mathematical tools and concepts developed in the study of chaotic systems, while these optical systems provide a new avenue for the investigation and demonstration of chaotic behavior. An interesting feature of this correspondence is that here chaos is not a nuisance, but in fact *essential* for effective optical memory.

Optical bistability arises when an optical system can have two stable output states for a single constant input,[1] and thus has a binary memory capability. It frequently arises from bistability in a material parameter ϕ (refractive index, temperature, photoexcitaton density, etc.) due to nonlinear coupling to the input optical beam(s). If ϕ relaxes and diffuses transversely, one can model such a system by a nonlinear partial differential equation[5]:

$$-l_D^2\nabla^2\phi+\tau\,\partial\phi/\partial t+\phi=f(\phi)I(\mathbf{r},t). \quad (1)$$

For large enough input intensity I, ϕ will be bistable provided the response function $f(\phi)$ is suitably nonlinear: e.g., Lorentzian (dispersive OB) or of step-function character (e.g., OB due to increasing absorption). An array of OB elements (pixels) can be defined by a suitable spatial modulation of $I(\mathbf{r})$, and individual pixels would be set high or low by suitable address pulses: I will not consider further the question of imposing binary patterns on the array and will assume henceforth that $I(\mathbf{r})$ is constant and spatially periodic, so defining an infinite array of identical pixels, with stationary states $\phi_s(\mathbf{r})$.

Memory states must be stable: Adding to ϕ_s a small perturbation $\psi(\mathbf{r})e^{\lambda t}$, we deduce from (1) that $\psi(\mathbf{r})$ obeys a Schrödinger-type equation:

$$[-l_D^2\nabla^2+V(\mathbf{r})]\psi=E\psi, \quad (2)$$

where

$$E=-(\lambda\tau+1)$$

and

$$V(\mathbf{r})=-I(\mathbf{r})f'(\phi_s(\mathbf{r})).$$

Stability of ϕ_s requires $\lambda<0$ for all solutions of (2), and so the ground state of (2) must have $E>-1$. Interesting configurations $\phi_s(\mathbf{r})$ include states which are *uniform* (all pixels "high" or "low"); *defect* (e.g., all but one low) and *random*; the corresponding Schrödinger problems are analogous to those of a crystal, a point defect, and an alloy, respectively.

The above model is applicable to two-dimensional optical memory arrays, but we now concentrate on the simpler one-dimensional case. In steady state, Eq. (1) is then analogous to a Newtonian mechanics problem, which is Hamiltonian and autonomous if $I(x)$ is constant, but generically chaotic[4] for $I(x)$ periodic, as in a pixel array. Anticipating that pixel independence will demand spacing $\geq l_D$, and knowing that "power per pixel" decreases with spot size,[6] we naturally make the approximation

$$I(x)=\sum_{n=-\infty}^{\infty}P\delta(x-nLl_D),$$

i.e., a δ-function array with spacing L diffusion lengths, corresponding to a kicked mechanical problem. The integration exactly between "kicks" yields a "stroboscopic map" for the values A_n of ϕ_s on the nth pixel:

$$2cA_n-sPf(A_n)-A_{n+1}-A_{n-1}=0, \quad (3)$$

where $c=\cosh L$, $s=\sinh L$. This equation can be interpreted as a nearest-neighbor coupling which decays exponentially with L: It thus probably captures the essential features of pixel coupling mechanisms more general than its antecedent model, while useful analogies with coupled-spin models may be anticipated for two-dimensional arrays.

A reversible, area-preserving mapping of the plane may be derived from (3), e.g., by our setting

$$B_n=A_{n-1} \text{ or } D_n=\tfrac{1}{2}(A_{n+1}-A_{n-1}) \quad (4)$$

leading to De Vogelaere maps[7] in the forms analyzed by Greene *et al.*[8] Physically, the (A,B) mapping generates the full pixel pattern ϕ_s from its value on the two neighboring pixels, while the (A,D) mapping does so from ϕ_s and its mean slope at a single pixel; I will use the (A,B) map here.

Uniform pixel excitation corresponds to a fixed point of the map:

$$f(A) = A\times 2(c-1)/sP = A\times 2\tanh(\tfrac{1}{2}L)/P = mA \quad (5)$$

which may be solved graphically, as in plane-wave OB problems—see Fig. 1.

The dynamical stability of these fixed points, or of any pixel pattern $\{A_n\}$, is governed by the linear mapping derived from (2). In the (A,B) representation, this map is given by the matrices

$$K_n(k) = \begin{bmatrix} T_n(k) & -1 \\ 1 & 0 \end{bmatrix},$$

where $k^2 = -E$ and

$$T_n(k) = 2\cosh kL - Pf'(A_n)\sinh kL/k.$$

The K_n act on a perturbation vector and $\{A_n\}$ will be unstable if there exists any such vector which remains bounded for all n, for some $k>1$. For a fixed point this requires $|T(k)|<2$ for some $k>1$. Stable fixed points thus obey $f'(A)=m$. Thus as in the plane-wave case, given three fixed points A_l, A_m, A_u, then A_l and A_u are stable, while the middle fixed point A_m is unstable.

Mapping stability of $\{A_n\}$ under M is also of interest. The Jacobian of M_n is $K_n(1)$, and since $K(1)>2$ for dynamically stable fixed points, such points are mapping unstable, in fact hyperbolic, as illustrated in Fig. 2. A_m is mapping stable (a center) for small L, surrounded by closed orbits. As L increases, however, A_m loses stability via a period-doubling sequence. *All* mapping-stable N-periodic sequences $\{A_n\}$ are dynamically unstable, because mapping stability implies

$$\mathrm{Tr}\left(\prod_{n=1}^{N} K_n(k)\right) < 2 \text{ for } k^2=1,$$

and thus, by continuity, for k^2 just bigger than 1, which implies dynamic instability.

The converse is not true, as noted above for A_m, but a restricted result is important: Any orbit $\{A_n\}$ for which $T_n(1)>2$ for all n is dynamically stable.[9] The argument is based on the fact that for $T_n(1)>2$, and *a fortiori* for $k>1$, a perturbation vector (ξ_n,η_n) gets trapped in a sector of the (ξ,η) plane in which $(\xi_n^2+\eta_n^2)$ is monotonic increasing as n either increases to ∞ or decreases to $-\infty$, or both. The condition $T(1)=2$ is valid at points for which $f'(A)=m$ (Fig. 1). All orbits which never stray into the "instability strip" between these points are dynamically stable and potentially useful memory states. Attention is drawn to similarities between the present problem and Frenkel-Kantorova models studied, e.g., by Aubry.[10] In particular Aubry's Theorem 4 seems applicable, and since it is easy to show that ξ_n has at most one sign change for $T_n(1)>2$, dynamic stability (strictly metastability in Aubry's terminology) follows.

The functional requirement of an optical memory is that it should have dynamically stable states $\{A_n\}$ representing arbitrary doubly infinite sets of binary digits —i.e., each pixel may be independently set high or low. Here I present the main results of this paper: useful lower bounds on pixel separation in such a device, some links with chaotic dynamics, and conditions on dynamical stability. The derivation uses the physical requirement of boundedness of $\{A_n\}$, together with an analogy

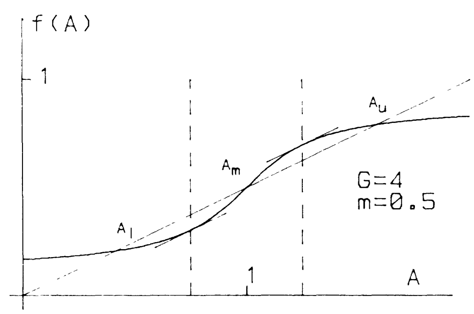

FIG. 1. Graphical determination of the uniform states of the OB array, given by the intersection with the response function $f(A)$ of a line of slope $m \sim P^{-1}$. The dashed vertical lines [defined by $f'(A)=m$] delineate the "instability strip"—states wholly outside the strip are dynamically stable. In the diagram, $f(A) = \{2+\arctan[G(A-1)]\}/4$.

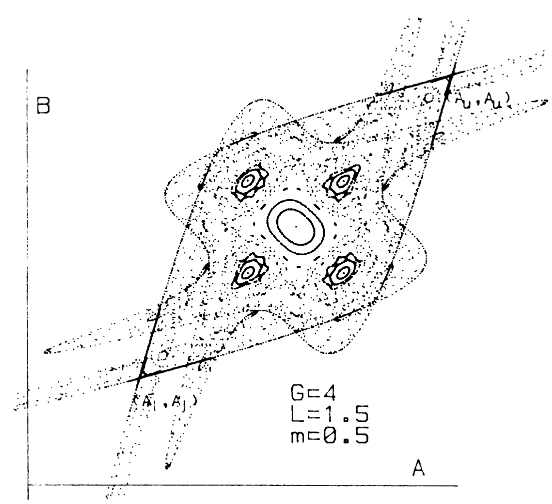

FIG. 2. Pattern of points generated by the map (5) for the response function of Fig. 1. Note closed orbits around $A_m=1$, while the other fixed points A_l, A_m are hyperbolic.

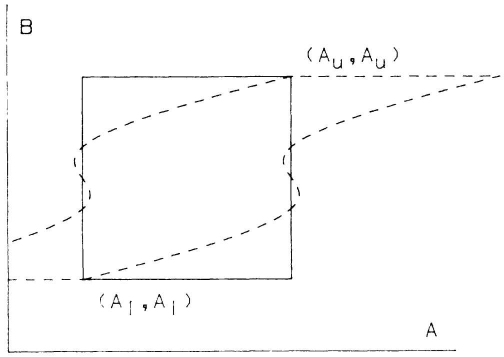

FIG. 3. Image of the square S_0 under the map (5) for small array spacing $L = 1.5$.

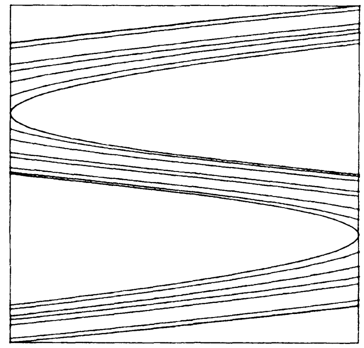

FIG. 4. For larger spacing the image intersects S_0 in three "stripes," whose own images are nine nested stripes.

between M and Smale's horseshoe map.[10] The argument can only be outlined here, but hyperbolicity can be proved in close analogy with the analysis in Chapter 5 of Guckenheimer and Holmes[11]; in particular, the conditions of the Smale-Birkhoff homoclinic theorem apply once S_1 has broken into three stripes.

Consider the square S_0:$A_l \le A,B \le A_u$. Every point outside S_0 escapes to infinity under iteration of M or M^{-1}. The set S of points bounded for all n is thus the intersection of all forward and inverse images of S_0:

$$S = \bigcap_{n=-\infty}^{\infty} M^n(S_0).$$

For small L, $S_1 = S_0 \cap M(S_0)$ is simply connected (Fig. 3), and of course contains all fixed points and closed orbits of M (Fig. 2). As the pixel separation is increased, however, S_1 breaks into two, then three disjoint "stripes" (Fig. 4). The images of these three stripes intersect S_0 in nine narrower stripes nested within S_1, and so forth. The limit for large n is a Cantor set of lines. Under M^{-1} each line breaks up into a Cantor set: S can thus be visualized as sets of nine infinitely nested "squares" (Fig. 5) which is itself a Cantor set topologically equivalent to the limit set of a double horseshoe (zigzag) map.[11]

Once S_1 breaks into three disjoint stripes, then given any doubly infinite string of binary digits Σ, S contains a point $(A,B)_\Sigma$, which generates under M a pixel pattern in 1:1 correspondence with Σ.[10] Starting at an arbitrary position in Σ I iterate M on S_0, selecting the upper or lower stripe according as the next digit of Σ is 1 or 0; I then map this stripe, and choose from its three image stripes the upper or lower according to the next digit of Σ, and so on, to arrive at a line uniquely determined by the right-hand portion of Σ. On application of the inverse map M^{-1} to this line the left portion generates a unique point $(A,B)_\Sigma$ as required. Thus, for example, two "corners" of S are the fixed points generating (. . .000.000. . .) and (. . .111.111. . .), while the other two corners generate (. . .000.111. . .) and (. . .11 1.000. . .).

The set of all Σ corresponds to a subset of S; the full set is generated by strings Σ' of ternary digits, by the relating of 2 to the middle stripe at each stage. M acts on S as a digit shift, and thus Σ and Σ' are invariant sets for M.[11]

The critical condition for stripe formation is that the image of the bottom (top) side of S_0 *touch* the left (right) side of S_0. This condition can be given a simple graphical interpretation: Let m_l (m_u) be the slope of the tangent from A_l (A_u) to $f(A)$ in Fig. 1, and let r be the smaller of the two ratios m_l/m, m_u/m. Then the critical pixel separation for stripe formation is L diffusion lengths, where

$$L = \ln[r + (2r-1)^{1/2}/(r-1)]. \tag{6}$$

Since $r \to 1$ as a switch point is approached (A_m collides with A_l or A_u), pixel independence for an array operated close to switching requires large spacing. Conversely, maximum pixel density is obtained when the operating point is chosen such that $m_l = m_u$, i.e., the two tangents are parallel.

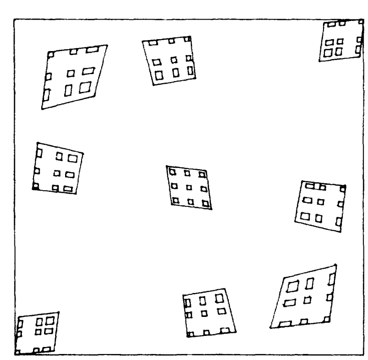

FIG. 5. Schematic illustration of the formation of the bounded set S as the limit of sets of nine nested "squares" formed by the intersection of the stripes of Fig. 3 with their inverse images.

S_0 is a convenient, but not optimal, starting figure for the generation of S: The "diamond" formed by the unstable and stable manifolds of A_l and A_u, discernible in Fig. 2, *is* optimal, since its boundaries contain subsets of S.

In nonlinear dynamics horseshoe formation is intimately associated with homoclinic tangencies and chaos[11]; this relates directly to the present problem, since the above-mentioned optimal condition for stripe formation is tangency of the stable and unstable manifolds of A_l and A_m, forming the point defects or homoclinic orbits (. . .0001000. . .) and (. . .1110111), respectively. The associated theory then guarantees the existence of periodic orbits of all periods as well as uncountable aperiodic orbits: This is precisely as required for, and illustrated by, the present model of an optical memory.

Effective optical memory demands that all members of Σ be dynamically stable. As noted above this is guaranteed if all A_n for each member lie outside the instability strip; this typically yields a minimum pixel spacing similar to that in (5). Conversely all sequences containing a 2 are unstable.[9] Closure of the gap between these two statements is possible for specific response functions; such cases as well as detailed justification of the present arguments will be elaborated elsewhere.[9]

In summary I have demonstrated in a simple case an intimate connection between optical memory and spatial chaos. On the one hand, the methods and concepts of nonlinear dynamics can yield rigorous results for basic and global features of optical memory function, while on the other hand the emphasis on mapping-unstable orbits and the additional question of dynamic stability may stimulate progress in nonlinear dynamics. Generalization to two-dimensional arrays and to related optical devices—such as image processors—and perhaps to other forms of memory device should prove rewarding.

This work was supported in part by the Stimulation Action Program of the European Community.

[1]H. M. Gibbs, *Optical Bistability—Controlling Light with Light* (Academic, New York, 1985).

[2]*From Optical Bistability Towards Optical Computing,* edited by P. Mandel, S. D. Smith, and B. S. Wherrett (North-Holland, Amsterdam, 1987), and Ref. 1.

[3]For example, Proc. Roy. Soc. London A **413**, 3–200 (1981).

[4]P. Coullet, C. Elphick, and D. Repaux, Phys. Rev. Lett. **58**, 431 (1987).

[5]W. J. Firth and I. Galbraith, IEEE J. Quantum Electron. **21**, 1399–1403 (1985).

[6]W. J. Firth, I. Galbraith, and E. M. Wright, J. Opt. Soc. Am. B **2**, 1005 (1985).

[7]R. De Vogelaere, in *Contributions to the Theory of Nonlinear Oscillations IV,* edited by S. Lefshetz, Annals of Mathematics Studies Vol. 41 (Princeton Univ. Press, Princeton, NJ, 1958), p. 53.

[8]J. M. Greene, R. S. MacKay, F. Vivaldi, and M. J. Feigenbaum, Physica (Amsterdam) **3D**, 468 (1981).

[9]W. J. Firth, to be published.

[10]S. Aubry, Physica (Amsterdam) **7D**, 240–258 (1983).

[11]J. Guckenheimer and P. Holmes, *Nonlinear Oscillations, Dynamical Systems, and Bifurcations of Vector Fields,* Applied Mathematical Sciences Vol. 42 (Springer-Verlag, Berlin, 1983).